Towards wideband mechanical metamaterials: Comparing nonlinear oscillator mechanisms

†*A. Banerjee^{1,2}, E.P. Calius², and R. Das¹

¹Department of Mechanical Engineering, University of Auckland, Auckland, New Zealand ²Callaghan Innovation, Auckland, New Zealand

*Presenting author: aban991@aucklanduni.ac.nz †Corresponding author: aban991@aucklanduni.ac.nz

Abstract

Metamaterial is a designed material, having some exotic phenomena in resonating frequency range, such as negative properties. This is often achieved through resonant electromagnetic, acoustic or mechanical structures inside the metamaterial. Mechanical metamaterials have a comprehensive range of applications in sound, vibration and seismic engineering. However, the effectiveness of metamaterials is limited to a relatively narrow frequency band as they are generally based on linear resonance mechanisms. These linear metamaterials do not perform well under the broadband excitation spectra that are common in real life applications. Towards the first step to widen the bandwidth of the metamaterial, different classes of nonlinear oscillations, namely Duffing type monostable and bistable, and piecewise linear, are studied in non-dimensional way and compared with each other, to identify the best one according to resonating bandwidth increment. A straightforward time history based iterative methodology FRSFTI is developed to get the frequency amplitude plot of a nonlinear system without employing any approximate perturbation method. The frequency-amplitude plot from this method shows a good agreement with the conventional perturbation method at the resonating frequency range; moreover, this method enables to compute the response away from the resonating range. From the analysis it can be concluded that the bandwidth increment of bistable Duffing type oscillator is largest compared to others.

Keywords: Nonlinear metamaterial, Mechanical metamaterial, Nonlinear oscillation, Bandwidth comparison, Multi-stability, Steady state response, Non-dimensional analysis

Introduction

Metamaterials are generalized composites that can exhibit unconventional behaviors and responses that are not commonly encountered in natural materials [Banerjee, B. (2011)], such as negative properties. This is often achieved through resonant electromagnetic [Lei, Z. (2008); Willis, J. R. (2011)], acoustic [Lee, S. H. et al. (2009); Huang, H. H. and Sun, C. T. (2012); Pai, P. F. et al. (2014); Sun, H. et al. (2014)] or mechanical structures inside the metamaterial. Mechanical metamaterials extensively used in the field of sound, vibration and seismic engineering. However, as they are generally based on linear resonance mechanisms, their effectiveness tends to be limited to a relatively narrow frequency band. These linear metamaterials do not perform well under the broadband excitation spectra that are common in real life applications.

Nonlinearity has a potential to widen the bandwidth of oscillator-based metamaterials by exploiting features, such as sub- and super-harmonic resonances, period multiplication, and chaotic response. Nonlinear metamaterials have already been studied in the context of electromagnetic wave propagation [Lapine, M. et al. (2014)], but to date the applicability of nonlinear metamaterials in other fields has received little attention. On the other hand, nonlinear oscillation and its effect on bandwidth have been well studied in the context of energy harvesting. Vibration of a ferromagnetic beam [Holmes, P. (1979); Moon, F. and Holmes, P. J. (1979); Erturk, A. and Inman, D. J. (2011)] or a beam with tip magnet [Stanton, S. C. et al. (2009); Zhou, S. et al. (2014)] in the presence of magnetic field can show monostable and bistable Duffing type oscillation depending on the position of magnets. Similarly, bistable and monostable oscillation can be found in the case of transverse [Sneller, A. J. et al. (2011); Cottone, F. et al. (2013); Andò, B. et al. (2014)] and axial [Masana, R. and Daqaq, M. F. (2012)] vibration

of post and pre-buckled beams, respectively. Transverse vibration of Euler spring systems [Winterflood, J. et al. (2002); Zhang, G. et al. (2013)] or inclined springs systems can also result in bistable oscillations. Comparative studies between bistable and monostable harvesters show that the output power and the bandwidth exhibited a greater increase during bistable chaotic response [Masana, R. and Daqaq, M. F. (2011); Daqaq, M. F. et al. (2014)]. Ferrari et al [Stanton, S. C. et al. (2010); Ferrari, M. et al. (2011)] have shown that as the slope of the inner wall of the potential well becomes steeper, the system performs like a monostable system, and the response of the system is reduced.

As a first step towards the development of a nonlinear mechanical metamaterial, the behaviors of three types of nonlinear oscillators are examined in non-dimensional form. The oscillators under consideration are characterized by the shape of their potential energy well, namely cubic monostable, cubic bistable, and piecewise linear, as shown in Figure 1.

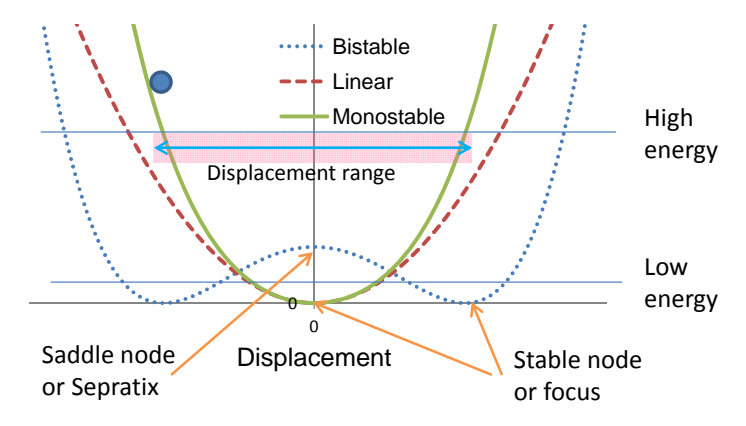


Figure 1 Potential well of typical bistable, monostable and linear system

Figure 1 shows that in a monostable system the potential well has only one stable point; whereas, the bistable system has two stable points and one saddle node. Displacement range is the peak to peak deflection of the system, as shown in Figure 1. It can be seen that the displacement range of a monostable resonator is less than that of linear and bistable oscillators, although due to the presence of sub- and super-harmonic resonances the monostable resonator can also generate a wider resonant bandwidth. On the other hand, the displacement range of a bistable oscillator is higher compared to other oscillators at high potential energy, but for lower energy vibration (below the sepratix), the displacement range is considerably reduced. The main objective of this paper is to investigate the effect of the steepness of the inner wall of the potential well and the relative distance between the stable nodes on the bandwidth for bistable systems and also compare that with monostable and piecewise type systems. The amplitude of the non-dimensional velocity in response to monochromatic excitation is determined and used to infer the bandwidth over which its response is greater than that of an equivalent linear oscillator. Thus, in this paper a comparative study is carried out to determine the bandwidth of monostable, bistable, piecewise linear system with that of a linear system.

Methodology

Linear oscillator

Equation of motion of linear oscillation can be written as

$$\ddot{u} + \omega^2 u = -\ddot{u}_g \sin \bar{\omega} t \tag{1}$$

where u and \ddot{u} are the displacement and acceleration of the system, \ddot{u}_g is the base excitation, ω and $\bar{\omega}$ are the natural frequency and excitation frequency of the system, respectively.

To non-dimensionalize Eq.(1), we set $u = Ax(\tau)$ and $t = \tau/\omega$. So, the modified Eq.(1) is

$$A\omega^{2} \frac{d^{2}x}{d\tau^{2}} + A\omega^{2}x = -\ddot{u}_{g} \sin\left(\frac{\overline{\omega}}{\omega}\tau\right)$$

$$\ddot{x} + x = -\sin(\eta\tau)$$
(2)

where
$$A = \frac{\ddot{u}_g}{\omega^2}$$
 and $\eta = \frac{\overline{\omega}}{\omega}$

Now, introducing a nonlinear stiffness term κ in Eq.(2) the nonlinear oscillation equation can be formulated.

Duffing type monostable cubic nonlinear system

Monostable Duffing oscillation is a common example of nonlinear oscillation. Vibration of a ferromagnetic beam under the influence of magnets [Ferrari, M. et al. (2010); Kang-Qi, F. et al. (2014)], axial and transverse vibration of a pre-buckled beam [Min, G.-B. and Eisley, J. G. (1972)] result in cubic monostable Duffing type nonlinearity. By introducing a nonlinear stiffness term κ in Eq.(2), the equation of motion of a typical monostable Duffing oscillator can be written as:

$$\ddot{u} + \omega^2 u + r\omega^2 u^3 = -\ddot{u}_\sigma \sin \bar{\omega} t \tag{3}$$

where r is ratio of the nonlinear spring constant to the linear spring constant. To non-dimensionalize Eq.(3), $u = Ax(\tau)$ and $t = \tau/\omega$ substitutions are considered. So, the modified form of Eq.(3) is:

$$A\omega^{2} \frac{d^{2}x}{d\tau^{2}} + A\omega^{2}x + r\omega^{2}A^{3}x^{3} = -\ddot{u}_{g} \sin\left(\frac{\overline{\omega}}{\omega}\tau\right)$$

$$\ddot{x} + x + \kappa x^{3} = -\sin(\eta\tau)$$
(4)

where $\kappa = rA^2 = r\frac{\ddot{u}_g^2}{\omega^4}$ shows that the non-dimensional nonlinear spring constant κ is directly

proportional to the ratio of nonlinear to linear spring constant and the square of the amplitude of the acceleration input, and inversely proportional to the fourth power of the natural frequency of the system.

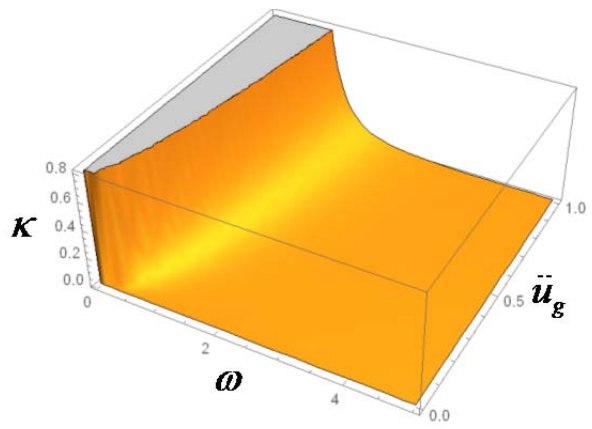


Figure 2 Plot of non-dimensional nonlinear spring constant (κ) with natural frequency (ω) and excitation amplitude (\ddot{u}_g) for a constant value of ratio of spring coefficient (r)

From Figure 2, it can be seen that the non-dimensional spring coefficient increases parabolically with the amplitude of vibration (\ddot{u}_g) , and is much higher at low natural frequencies.

The restoring non-dimensional force (F) and potential energy (U) can be expressed as:

$$F(x) = x + \kappa x^3$$

$$U(x) = \int_0^x F(x) dx = \frac{1}{2} x^2 + \frac{\kappa}{4} x^4$$
(5)

Duffing type bistable cubic nonlinear system

Bistable Duffing oscillation is another common form of nonlinear oscillation. Vibration of ferromagnetic beam under the influence of magnets [Stanton, S. C., McGehee, C. C. et al. (2010); Ferrari, M., Baù, M. et al. (2011)], axial and transverse vibration of post-buckled beam [Virgin, L. and Davis, R. (2003); Ibrahim, R. A. (2008); Camescasse, B. et al. (2013)], vibration of Euler spring system [Winterflood, J., Barber, T. A. et al. (2002); Ibrahim, R. A. (2008); Huang, X. et al. (2014)], result in cubic bistable Duffing type nonlinearity. Unlike monostable oscillation, bistable Duffing equation has two stable nodes and one saddle node. The non-dimensional bistable Duffing equation can be written as:

$$\ddot{x} - x + \kappa x^3 = -\sin(\eta \tau) \tag{6}$$

So the restoring force (F) and the potential energy (U) can be expressed as:

$$F(x) = -x + \kappa x^{3}$$

$$U(x) = \int F(x) dx = -\frac{1}{2}x^{2} + \frac{\kappa}{4}x^{4} + c$$
(7)

Now at the stable nodes the restoring force must be 0. So, the location of the stable node can be calculated as $x_{eq} = \pm \sqrt{\frac{1}{\kappa}}$. If the minimum value of potential well is assumed to be zero, then the value of c is:

$$U\left(\pm\sqrt{\frac{1}{\kappa}}\right) = -\frac{1}{2}\frac{1}{\kappa} + \frac{\kappa}{4}\frac{1}{\kappa^2} + c = 0 \to c = \frac{1}{4\kappa}$$
 (8)

The different shapes of the potential well are plotted for various values of κ .

Piecewise linear system

In the piecewise linear system, the restoring force varies with the distance linearly up to a certain range. Thereafter due to impact with stopper, the slope of the restoring force curve changes significantly, but still remains linear. As the restoring force curve consists of different straight lines, this type of system is commonly known as a piecewise linear system. Vibro-impacting devices [Soliman, M. S. M. et al. (2008); Vandewater, L. and Moss, S. (2013)], where stoppers are placed at some distance from the stable point of the beam, are an example of this type of oscillator. The impact between the stopper and the beam creates the nonlinear term. The equation of motion of piecewise linear system can be written as:

$$\ddot{u} + \omega^2 u = -\ddot{u}_g \sin(\eta \tau); u + \tilde{g} \ge 0$$
(9)

The Eq.(9) can be written in non-dimensional form by considering, $u = Ax(\tau)$, $t = \tau/\omega$ and

$$\tilde{g} = g \frac{\ddot{u}_g}{\omega^2}.$$

$$\ddot{x} + x = -\sin(\eta \tau); \quad x + g \ge 0 \tag{10}$$

The restoring force (F) and the potential energy (U) can be expressed as:

$$F(x) = \begin{cases} x & x+g \ge 0 \\ \infty & x+g < 0 \end{cases}$$

$$U(x) = \begin{cases} \frac{x^2}{2} & x+g \ge 0 \\ \infty & x+g < 0 \end{cases}$$
(11)

Identification of parameter

To compare the bandwidth of these different systems, their frequency response must be computed for a range of oscillator parameters. In linear systems, the amplitude corresponding to a specific excitation frequency of motion is conventionally solved because this is sufficient to completely describe the vibration. On the other hand, as there may be no linear correlation among all the parameters in nonlinear systems, displacement amplitude does not fully describe the oscillator dynamics. In this paper, the non-dimensional velocity amplitude $\max(\dot{x})$ is used to describe the response, because it can represent not only the maximum velocity, but also the maximum momentum and the maximum kinetic energy of the system, which have greater significance in the context of metamaterials. The amplitude of the velocity of monochromatic excitation of frequency

$$(\omega)$$
 is (u_g/ω) , which results the input momentum of the system (P_s) is $\frac{M\ddot{u}_g}{\omega}$. The non-

dimensional momentum (P) of the system can be expressed as the ratio of the momentum $(\tilde{P} = M\dot{u})$ and the input momentum corresponding to system (P_s) , in Eq.(12).

$$P = \frac{\tilde{P}}{P_s} = \frac{M\dot{u}\omega}{M\ddot{u}_g} = \frac{A\omega\dot{x}\omega}{\ddot{u}_g} = \dot{x}$$
 (12)

Solution

The frequency content of a signal is generally a more important parameter than its time history, because the corresponding response to a particular frequency can be easily calculated by convolution. In linear systems Fourier transformation of the equation of motion produces its frequency response directly; whereas in nonlinear systems Fourier transformation is not applicable [Cameron, T. M. and Griffin, J. H. (1989)]. In order to determine the frequency response of a nonlinear system, several methods have been developed mainly based on perturbation techniques. The harmonic balance (HB) method [Nayfeh, A. H. and Mook, D. T. (2008)] is the most popular and widely used technique to determine the frequency response of a nonlinear system [Beléndez, A. et al. (2007); Beléndez, A. et al. (2009); Cochelin, B. and Vergez, C. (2009); Wang, X. et al. (2012); García-Saldaña, J. D. and Gasull, A. (2013); Karkar, S. et al. (2013)]. The HB method is adequate where only single harmonic description is sufficient, as it is in the case of weakly nonlinear systems. Among the techniques that can deal with strong nonlinearity, alternating frequency/time (AFT) method [Cameron, T. M. and Griffin, J. H. (1989)], homotopy method [Liao, S. (2004); Vyasarayani, C. P. et al. (2012)] and the max-min method [He, J.-H. (2008); Azami, R. et al. (2009); Ibsen, L. B. et al. (2010)] have gained popularity.

In this paper a simple time domain based iterative method, an in house program (FRSFTI), is developed to compute the frequency response of a particular nonlinear system. To apply the method, a frequency domain of interest needs to be first defined. The program FRSFTI enables the user to control the number of steps and discretize the frequency domain into finite number of input excitation frequencies. Sinusoidal excitation of each frequency is applied to a specific system to calculate its response. To reduce the frequency leakage and the aliasing, a sine wave of fifty cycles is considered in the analysis [Lynch, S. (2011)]. The ODE45 solver of MATLAB version 8.4

[Mathworks, Natick, MA] is used to solve the equation of motion for a particular monochromatic excitation. An event identifier is amalgamated with the ODE in response to the case of a piece-wise linear system, to locate the occurrence of impact and restart integration with new initial values. Then, maximum of velocity $(\max(\dot{x}))$ is plotted for the corresponding frequency to obtain the frequency response because according to Eq.(12) it can represent the non-dimensional momentum which is the most important parameter in metamaterial. As the method is based on time domain solutions, there are certain advantages of this method over existing methods, such as

- No stabilization check is required and it results in a single output for a particular frequency; whereas the HB method results in a sixth order correlation between the amplitude and frequency. [Nayfeh, A. H. and Mook, D. T. (2008)].
- It can solve any type of nonlinearity or discontinuity; whereas perturbation methods are approximate and sometimes cannot deal with high level of nonlinearity or discontinuity [Nayfeh, A. H. and Mook, D. T. (2008)].
- As every frequency excitation is applied to the system, the method can work in every frequency range; whereas, most of the perturbation methods can only work near the resonating frequency or some specific sub or super harmonics.
- The method is programmable, so rigorous mathematical calculations are not needed.

To compare the bandwidth increment of three different classes of nonlinear oscillators, in each case the initial condition is assumed to be the stable node to ensure the initial potential energy is zero. That is why, initial condition is assumed to be (0,0) for the linear, monostable and piecewise linear system; whereas for bistable condition the initial condition is $(\pm \sqrt{1/\kappa}, 0)$. Maximum non-dimensional velocity $\max(\dot{x})$ is considered as the comparing parameter. Figure 3 shows the flow chart of the full process.

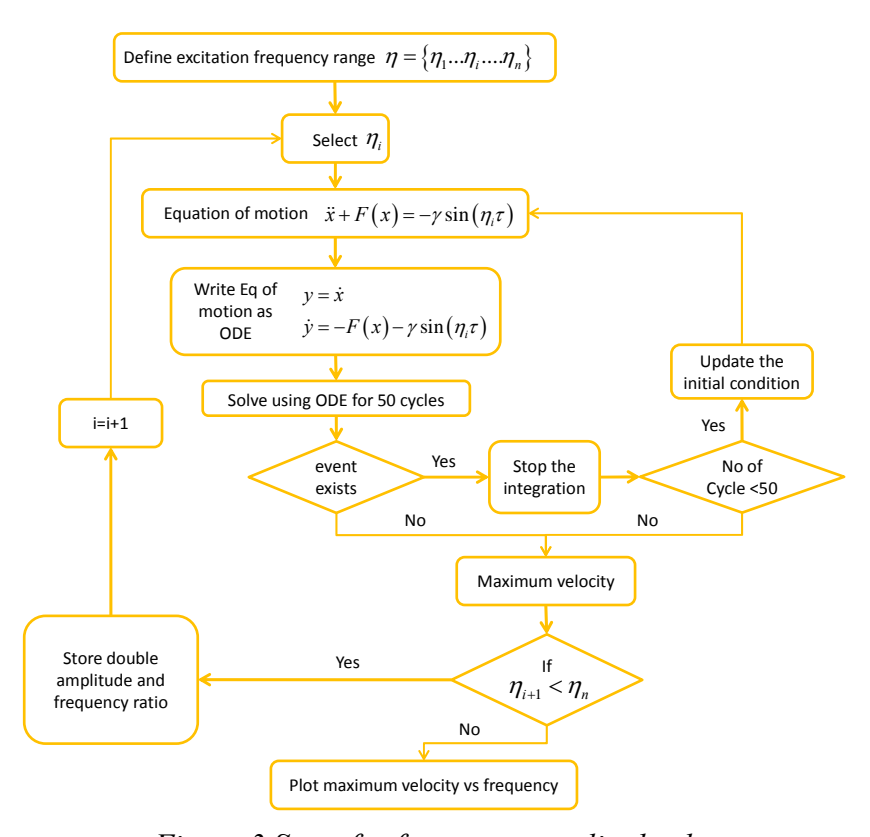


Figure 3 Steps for frequency-amplitude plot

Results and Discussions

Monostable cubic nonlinear system

The potential well and the restoring force profile of the monostable system for varying nonlinearity is plotted in Figure 4, based on Eq.(5).

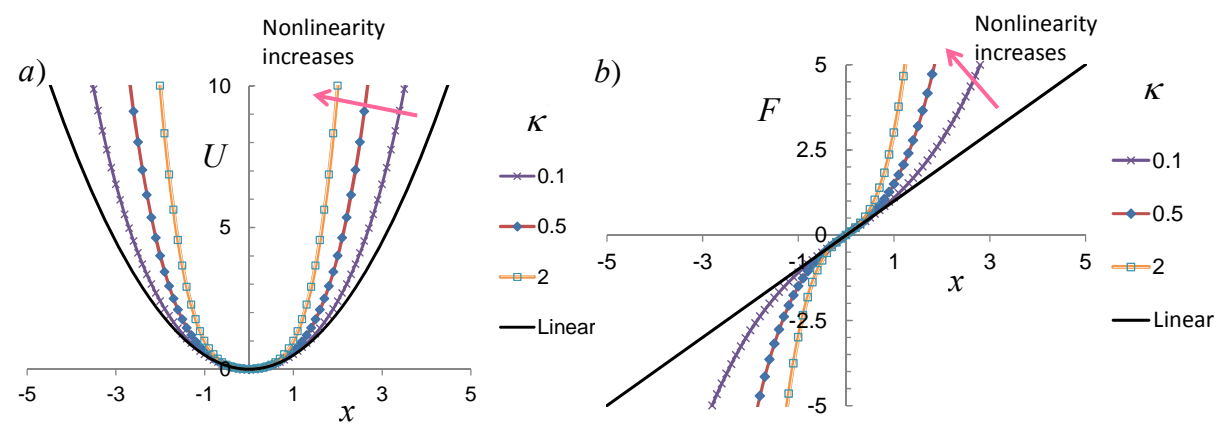


Figure 4 a) Potential energy well and b) restoring force of a linear and a monostable cubic nonlinear system for three level of nonlinearity

Figure 4 shows the variation of potential energy and the restoring force of a linear and a monostable cubic nonlinear system for three different levels of nonlinearity. The potential well becomes steeper and the restoring force shows hardening behavior as the nonlinearity increases. The resulting frequency response is shown in Figure 5.

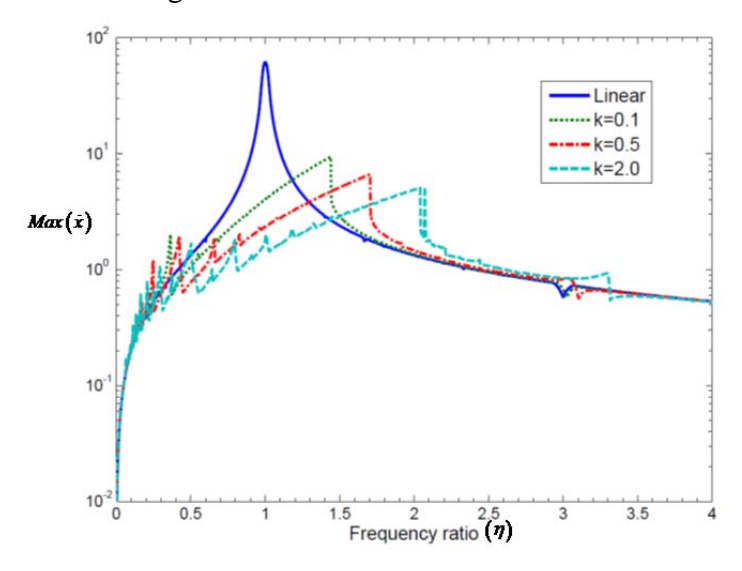


Figure 5 Frequency response of the maximum non-dimensional velocity (\dot{x}) that relates to the amplitude of non-dimensional momentum of linear and monostable systems of varying nonlinearity

From Figure 5 it can be concluded that the resonance peak shifts to a higher side and its amplitude reduces as nonlinearity increases. Due to the presence of sub and super harmonic resonances, amplification is observed in the low frequency range. The frequency response of monostable systems is generally less than the equivalent linear system.

Bistable cubic nonlinear system

The potential well and the restoring force profile of bistable system for varying nonlinearity is plotted in Figure 6, based on Eq.(7).

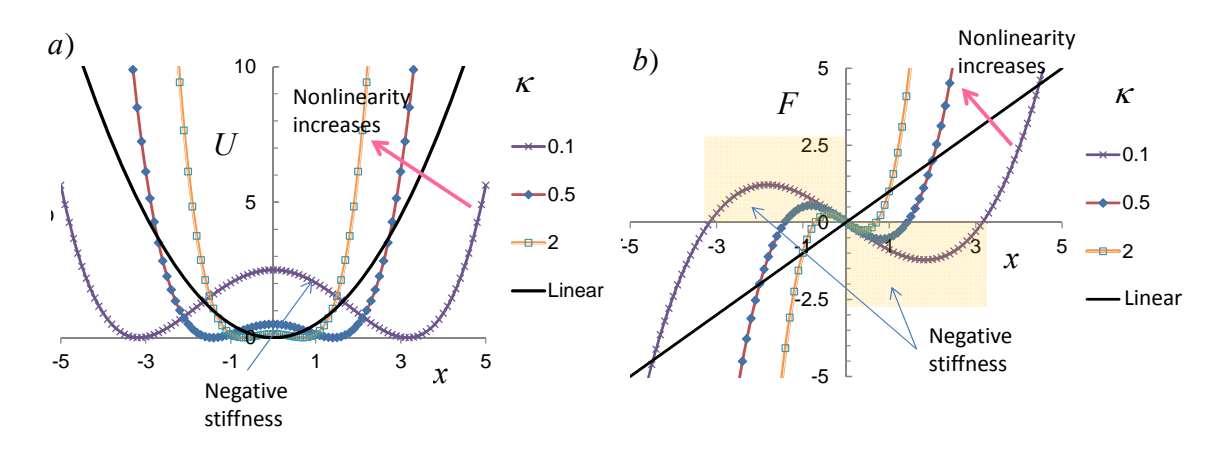


Figure 6 a) Potential energy well and b) restoring force of a linear and a monostable cubic nonlinear system for three levels of nonlinearity

Figure 6 shows the variation of potential energy and the restoring force of a linear and a bistable cubic nonlinear system for three different levels of nonlinearity. It can be noted that the stable nodes approach closer with increasing level of nonlinearity. Negative stiffness resulted at the region between two stable nodes as shown in Figure 6. The distance between the outer walls of potential wells decreased with increment of nonlinearity, hence the motion confined between two walls. Simultaneously, the energy required to overcome the sepratix barrier decreases with nonlinearity, which enables the motion to overcome the sepratix barrier easily and results a bistable motion. Therefore, an optimum level of nonlinearity should exist where the maximum response can be obtained in the case of bistable systems.

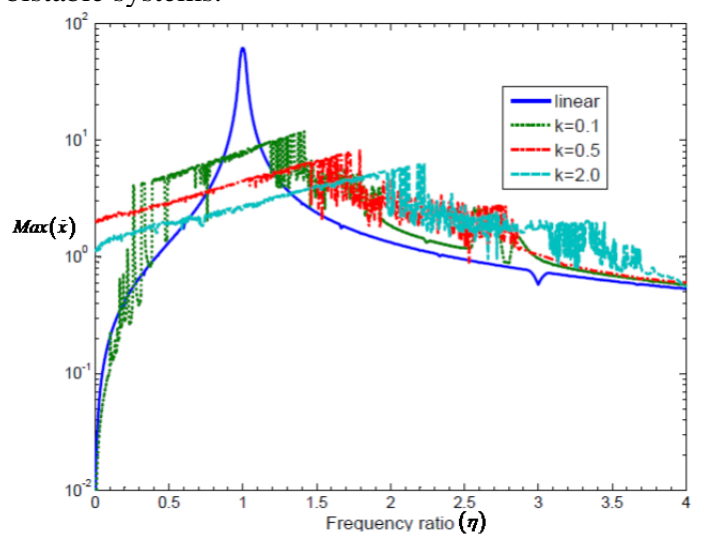


Figure 7 Frequency response of the maximum non-dimensional velocity (\dot{x}) that relates to the amplitude of non-dimensional momentum of linear and bistable systems of varying nonlinearity

Figure 7 shows that the nonlinear system's response (maximum non-dimensional velocity) is above the equivalent linear response over a considerable range of frequencies. The increased response is particularly marked at low frequencies, which of significant practical interest, and upon examination this frequency range is found to be greatest for $\kappa = 0.5$ among the three nonlinear systems. Bistable systems with high nonlinearity show much higher response in the low frequency range because the energy required to cross the sepratix barrier is less.

Piecewise linear system

The potential well and the restoring force profile of piecewise linear system for varying gap distance is plotted in Figure 8, based on Eq.(11).

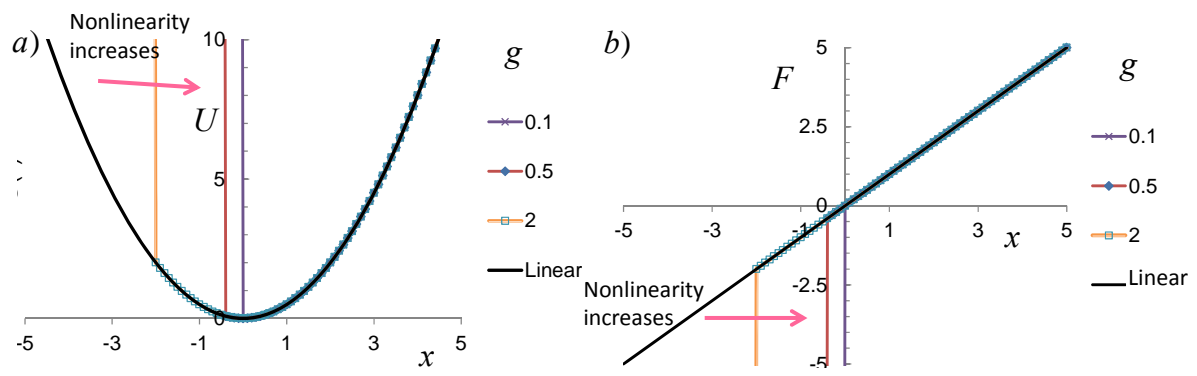


Figure 8 a) Potential energy well and b) restoring force of a linear and a piecewise linear system for three level of nonlinearity

Figure 8 shows that the potential well and the restoring force of a piecewise linear system, such as a vibro-impacting device, are the same as those for a linear system until the point of impact, whereupon a large impacting force is suddenly applied.

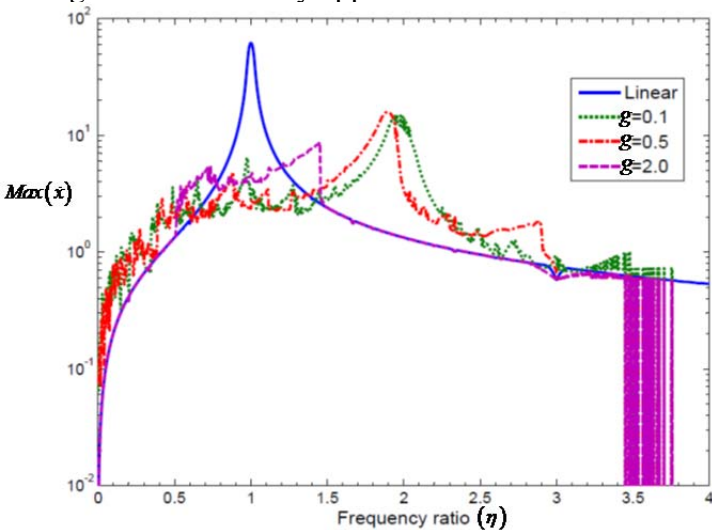


Figure 9 Frequency response of the maximum non-dimensional velocity (\dot{x}) which represents the amplitude of non-dimensional momentum of linear and bistable systems of varying nonlinearity

Figure 9 shows that the nonlinear system's response (maximum non-dimensional velocity) is above the equivalent linear response over a considerable range of frequencies. Figure 9 shows a remarkable increase in the frequency response at low frequency range and at a frequency ratio (η) around 2. Due to the impact, the motion path reduces which shifts the frequency towards $\eta = 2$. When the displacement of the system is more than the gap distance then impact happens, otherwise for non-impacting case the frequency response curve follows the linear response curve. That is why the systems having large gap yields very less bandwidth and almost follows the linear path.

Bandwidth

To compare the bandwidth of these three nonlinear systems considered with that of an equivalent linear system, the frequency range is divided into two main categories: the low range when the frequency ratio is below the linear resonant frequency ($\eta < 1$), and the high range when the

frequency ratio is above the linear resonant frequency ($\eta > 1$). The low and high ranges are further subdivided into two parts, the nonlinearity dominated range (NLD) and the linearity dominated range (LD). In the NLD range, the maximum momentum of the nonlinear system is greater than that of the linear one; whereas, in the LD range the linear response is higher than the nonlinear one. A bandwidth index (BWI) for each system at different ranges, such as low, high and overall, is calculated based on the ratio:

$$BWI = \frac{NLD}{LD} \tag{13}$$

The bandwidth comparison of all the proposed systems is given in Table 1.

Table 1 Summary of nonlinearity-dominated frequency range (non-dimensional) and the associated bandwidth index (BWI) for three different types of nonlinear systems

Type of	Level of	Frequency band increment					
nonlinearity	nonlinearity	Low range		High range		Overall	
		NLD (η)	BWI	NLD (η)	BWI	NLD (η)	BWI
Monostable	$\kappa = 0.1$	0.28	0.39	2.02	2.06	2.30	1.31
	$\kappa = 0.5$	0.27	0.37	1.86	1.63	2.13	1.14
	$\kappa = 2.0$	0.20	0.25	1.88	1.67	2.08	1.08
Bistable	$\kappa = 0.1$	0.57	1.34	2.86	19.83	3.43	5.99
	$\kappa = 0.5$	0.76	3.10	2.78	12.89	3.54	7.70
	$\kappa = 2.0$	0.63	1.69	2.67	8.15	3.30	4.71
Piecewise	g = 2.0	0.69	2.25	1.07	0.55	1.76	0.79
	g = 0.5	0.62	1.66	1.64	1.21	2.27	1.31
	g = 0.1	0.65	1.87	1.94	1.84	2.60	1.85

Remarks

From the above discussion the following remarks can be made:

- The relative magnitude of the nonlinear term is proportional to the square of amplitude of excitation and the ratio of nonlinear to linear stiffness, and inversely proportional to the forth power of natural frequency of the system. The strength of the nonlinearity increases rapidly as the frequency of excitation decreases.
- In a monostable system, the potential well becomes stiffer with increasing nonlinearity. The nonlinearity dominated bandwidth in the low frequency range is lower than that of the linear system and much lower than that of the other nonlinear systems, such as bistable and piecewise linear.
- In a bistable system, the energy required to overcome the sepratix decreases and the stable nodes approach closer as nonlinearity increases. This lowers the threshold to achieve the bistable response that produces maximum displacement and velocity in the low frequency excitation. On the other hand, the potential well becomes narrower and steeper, which reduces the velocity peak. For this reason, the nonlinearity dominated bandwidth increases up to an optimum value and thereafter it decreases.
- A piecewise linear system having large gap size results least nonlinear dominated bandwidth, but the bandwidth increases significantly as the gap reduces.

Conclusion

In this paper, a comparative study of three types of nonlinear systems, namely, cubic monostable and bistable, and piecewise linear, is carried out using non-dimensional variables. The equations of motion for these systems were non-dimensionalized and solved numerically for monochromatic

excitation over a range of frequencies. To examine the effect of nonlinearity on the response bandwidth, the non-dimensional velocity response of these systems is compared to that of a linear system. A new parameter, bandwidth index (BWI), is proposed and used to quantify the relative performance of these nonlinear systems. Of the three systems studied, the bistable system with intermediate nonlinearity has the largest nonlinear dominated bandwidth (NLD) and BWI, both for low range and overall.

References

- Andò, B., Baglio, S., Bulsara, A. R. and Marletta, V. (2014). A bistable buckled beam based approach for vibrational energy harvesting Sensors and Actuators A: Physical **211**(0): 153-161.
- Azami, R., Ganji, D. D., Babazadeh, H., Dvavodi, A. G. and Ganji, S. S. (2009). He's Max–Min Method for the relatistic oscillator and high order Duffing equation International Journal of Modern Physics B **23**(32): 5915-5927.
- Banerjee, B. (2011). An Introduction to Metamaterials and Waves in Composites, Auckland, Taylor & Fransis.
- Beléndez, A., Gimeno, E., Alvarez, M. L. and Méndez, D. I. (2009). Nonlinear oscillator with discontinuity by generalized harmonic balance method Computers & Mathematics with Applications **58**(11–12): 2117-2123.
- Beléndez, A., Hernández, A., Beléndez, T., Álvarez, M. L., Gallego, S., Ortuño, M. and Neipp, C. (2007). Application of the harmonic balance method to a nonlinear oscillator typified by a mass attached to a stretched wire Journal of Sound and Vibration **302**(4–5): 1018-1029.
- Cameron, T. M. and Griffin, J. H. (1989). An Alternating Frequency/Time Domain Method for Calculating the Steady-State Response of Nonlinear Dynamic Systems Journal of Applied Mechanics **56**(1): 149-154.
- Camescasse, B., Fernandes, A. and Pouget, J. (2013). Bistable buckled beam: Elastica modeling and analysis of static actuation International Journal of Solids and Structures **50**(19): 2881-2893.
- Cochelin, B. and Vergez, C. (2009). A high order purely frequency-based harmonic balance formulation for continuation of periodic solutions Journal of Sound and Vibration **324**(1–2): 243-262.
- Cottone, F., Basset, P., Vocca, H., Gammaitoni, L. and Bourouina, T. (2013). Bistable electromagnetic generator based on buckled beams for vibration energy harvesting Journal of Intelligent Material Systems and Structures: 1045389X13508330.
- Cottone, F., Gammaitoni, L., Vocca, H., Ferrari, M. and Ferrari, V. (2012). Piezoelectric buckled beams for random vibration energy harvesting Smart materials and structures **21**(3): 035021.
- Daqaq, M. F., Masana, R., Erturk, A. and Dane Quinn, D. (2014). On the Role of Nonlinearities in Vibratory Energy Harvesting: A Critical Review and Discussion Applied Mechanics Reviews **66**(4): 040801-040801.
- Erturk, A. and Inman, D. J. (2011). Broadband piezoelectric power generation on high-energy orbits of the bistable Duffing oscillator with electromechanical coupling Journal of Sound and Vibration **330**(10): 2339-2353.
- Ferrari, M., Baù, M., Guizzetti, M. and Ferrari, V. (2011). A single-magnet nonlinear piezoelectric converter for enhanced energy harvesting from random vibrations Sensors and Actuators A: Physical **172**(1): 287-292.
- Ferrari, M., Ferrari, V., Guizzetti, M., Andò, B., Baglio, S. and Trigona, C. (2010). Improved energy harvesting from wideband vibrations by nonlinear piezoelectric converters Sensors and Actuators A: Physical **162**(2): 425-431.
- García-Saldaña, J. D. and Gasull, A. (2013). A theoretical basis for the Harmonic Balance Method Journal of Differential Equations **254**(1): 67-80.
- He, J.-H. (2008). Max-min approach to nonlinear oscillators International Journal of Nonlinear Sciences and Numerical Simulation 9(2): 207-210.
- Holmes, P. (1979). A nonlinear oscillator with a strange attractor Philosophical Transactions of the Royal Society of London. Series A, Mathematical and Physical Sciences **292**(1394): 419-448.
- Huang, H. H. and Sun, C. T. (2012). Anomalous wave propagation in a one-dimensional acoustic metamaterial having simultaneously negative mass density and Young's modulus The Journal of the Acoustical Society of America 132: 2887.
- Huang, X., Liu, X., Sun, J., Zhang, Z. and Hua, H. (2014). Vibration isolation characteristics of a nonlinear isolator using Euler buckled beam as negative stiffness corrector: A theoretical and experimental study Journal of Sound and Vibration **333**(4): 1132-1148.
- Ibrahim, R. A. (2008). Recent advances in nonlinear passive vibration isolators Journal of Sound and Vibration **314**(3–5): 371-452.
- Ibsen, L. B., Barari, A. and Kimiaeifar, A. (2010). Analysis of highly nonlinear oscillation systems using He's max-min method and comparison with homotopy analysis and energy balance methods Sadhana **35**(4): 433-448.
- Kang-Qi, F., Chun-Hui, X., Wei-Dong, W. and Yang, F. (2014). Broadband energy harvesting via magnetic coupling between two movable magnets Chinese Physics B 23(8): 084501.

- Karkar, S., Cochelin, B. and Vergez, C. (2013). A high-order, purely frequency based harmonic balance formulation for continuation of periodic solutions: The case of non-polynomial nonlinearities Journal of Sound and Vibration **332**(4): 968-977.
- Lapine, M., Shadrivov, I. V. and Kivshar, Y. S. (2014). Colloquium: Nonlinear metamaterials Reviews of Modern Physics **86**(3): 1093.
- Lee, S. H., Park, C. M., Seo, Y. M., Wang, Z. G. and Kim, C. K. (2009). Acoustic metamaterial with negative density Physics Letters A 373(48): 4464-4469.
- Lei, Z. (2008). Effective 1-D material properties of coplanar-waveguide-based EBG- and meta-materials, Metamaterials, 2008 International Workshop on.
- Liao, S. (2004). On the homotopy analysis method for nonlinear problems Applied Mathematics and Computation 147(2): 499-513.
- Lynch, S. (2011). MATLAB Programming for Engineers, Applications of Chaos and Nonlinear Dynamics in Engineering-Vol. 1, Springer: 3-35.
- Masana, R. and Daqaq, M. F. (2011). Electromechanical modeling and nonlinear analysis of axially loaded energy harvesters Journal of Vibration and Acoustics **133**(1): 011007.
- Masana, R. and Daqaq, M. F. (2011). Relative performance of a vibratory energy harvester in mono- and bi-stable potentials Journal of Sound and Vibration **330**(24): 6036-6052.
- Masana, R. and Daqaq, M. F. (2012). Energy harvesting in the super-harmonic frequency region of a twin-well oscillator Journal of Applied Physics 111(4): -.
- Min, G.-B. and Eisley, J. G. (1972). Nonlinear Vibration of Buckled Beams Journal of Manufacturing Science and Engineering **94**(2): 637-645.
- Moon, F. and Holmes, P. J. (1979). A magnetoelastic strange attractor Journal of Sound and Vibration **65**(2): 275-296. Nayfeh, A. H. and Mook, D. T. (2008). Nonlinear oscillations, John Wiley & Sons.
- Pai, P. F., Peng, H. and Jiang, S. (2014). Acoustic metamaterial beams based on multi-frequency vibration absorbers International Journal of Mechanical Sciences **79**: 195-205.
- Sneller, A. J., Cette, P. and Mann, B. P. (2011). Experimental investigation of a post-buckled piezoelectric beam with an attached central mass used to harvest energy Proceedings of the Institution of Mechanical Engineers. Part I: Journal of Systems and Control Engineering 225(4): 497-509.
- Soliman, M. S. M., El-Saadany, E. M., Mansour, E. F. and Abdel-Rahman, R. R. (2008). A wideband vibration-based energy harvester Journal of Micromechanics and Microengineering **18**(11).
- Stanton, S. C., McGehee, C. C. and Mann, B. P. (2009). Reversible hysteresis for broadband magnetopiezoelastic energy harvesting Applied Physics Letters **95**(17): 174103.
- Stanton, S. C., McGehee, C. C. and Mann, B. P. (2010). Nonlinear dynamics for broadband energy harvesting: Investigation of a bistable piezoelectric inertial generator Physica D: Nonlinear Phenomena **239**(10): 640-653.
- Sun, H., Yan, F., Gu, H. and Li, Y. (2014). Acoustic metamaterial with negative parameter, Proceedings of SPIE The International Society for Optical Engineering.
- Vandewater, L. and Moss, S. (2013). Probability-of-existence of vibro-impact regimes in a nonlinear vibration energy harvester Smart Materials and Structures **22**(9): 094025.
- Virgin, L. and Davis, R. (2003). Vibration isolation using buckled struts Journal of Sound and Vibration **260**(5): 965-973.
- Vyasarayani, C. P., Uchida, T. and McPhee, J. (2012). Single-shooting homotopy method for parameter identification in dynamical systems Physical Review E **85**(3): 036201.
- Wang, X., Li, C., Huang, T. and Duan, S. (2012). Predicting chaos in memristive oscillator via harmonic balance method Chaos: An Interdisciplinary Journal of Nonlinear Science **22**(4): 043119.
- Willis, J. R. (2011). Effective constitutive relations for waves in composites and metamaterials Proceedings of the Royal Society A: Mathematical, Physical and Engineering Science **467**(2131): 1865-1879.
- Winterflood, J., Barber, T. A. and Blair, D. G. (2002). Mathematical analysis of an Euler spring vibration isolator Physics Letters A **300**(2–3): 131-139.
- Zhang, G., Zhu, X., Xu, R. and Li, T. (2013). Vibration isolation characteristics of euler strut spring used in low frequency vibration isolation system. **248**: 475-480.
- Zhou, S., Cao, J., Inman, D. J., Liu, S. and Wang, Z. (2014). Broadband tristable energy harvester: Modeling and experiment verification Applied Energy **133**(0): 33-39.